Front. Optoelectron. 2015, 8(1): 44–56
DOI 10.1007/s12200-014-0439-x

REVIEW ARTICLE

Tailoring electromagnetic responses in terahertz superconducting metamaterials

Xiaoling ZHANG, Jianqiang GU (✉), Jiaguang HAN (✉), Weili ZHANG

Center for Terahertz Waves and College of Precision Instrument and Optoelectronics Engineering, Tianjin University, and the Key Laboratory of Optoelectronics Information and Technology (Ministry of Education), Tianjin 300072, China

Abstract Superconducting terahertz metamaterials have attracted significant interest due to low loss, efficient resonance switching and large-range frequency tunability. The super conductivity in the metamaterials dramatically reduces ohmic loss and absorption to levels suitable for novel devices over a broad range of electromagnetic spectrum. Most metamaterials utilize subwavelength-scale split-ring resonators as unit building blocks, which are proved to support fundamental inductive-capacitive resonance, to achieve unique resonance performance. We presented a review of terahertz superconducting metamaterials and their implementation in multifunctional devices. We began with the recent development of superconducting metamaterials and their potential applications in controlling and manipulating terahertz waves. Then we explored the tuning behaviors of resonance properties in several typical, actively controllable metamaterials through integrating active components. Finally, the ultrafast dynamic nonlinear response to high intensity terahertz field in the superconducting metamaterials was presented.

Keywords superconducting metamaterial, terahertz, active metamaterial

1 Introduction

Metamaterials (MMs) termed as artificial composite structures exhibiting exotic electromagnetic properties not possessed by natural material, have aroused enormous interest in recent years. MMs exploited to achieve negative refraction was first proposed by Veselago in1968, who demonstrated that materials ingeniously possessing negative permittivity ε and permeability μ would have negative refractive index without breaking the existing physical laws. Until now, MMs have become a class of newly developed artificial composites with various novel electromagnetic performances. A lot of novel concepts and intriguing devices have been verified and investigated based on MMs, such as super lens [1,2], negative refraction [3], plasmon induced transparency [4], novel optical activities [5], and invisibility cloaking [6,7], etc. The novel characteristics of MMs not only reveal a deep understanding of fundamental science behind but also push an important step toward nonlinear and quantum MM devices which are difficult or impossible to achieve via conventional approaches.

Until now, MMs have generally adapted high conductive metallic elements patterned on dielectric substrates to implement responses to incident electric and/or magnetic fields. However, the intrinsic ohmic absorption in metals prohibits MMs' promotion toward novel functional devices, particularly in the frequency regimes higher than the microwave band. Besides, the intrinsic effective permittivity and permeability of metals are hardly influenced by external stimulation. Therefore, active manipulation of the MM response has to introduce additional material elements which not only increase the fabrication difficulty but also lower down the performance of the multifunctional devices. One approach to solve these problems is the use of superconductors (SCs) instead of metals. Contrary to metals, the resistance of SCs may fall down to zero under particular situation, resulting in an extreme increment of the figure of merit (FOM) in MMs. In addition, behaviors control of superconducting MMs, including resonance frequency shift and transmitted amplitude modulation, can be achieved through various methods as the superconductivity exhibits a strong dependence on ambient situation [8]. In 2005, Ricci et al. demonstrated the negative refraction index in the microwave regime with a MM made from low-loss dielectric substrate and SC mental Niobium (Nb), which for the first time introduced SCs into the MM research [9].

Received April 25, 2014; accepted June 13, 2014

E-mail: gjq@tju.edu.cn, jiaghan@tju.edu.cn

Since then, majority of initial studies on SC MMs have been carried out at microwave frequencies, where metals already show good conductivity for most devices. Thus recently, focus has been moved to the higher frequency regime [10], particular terahertz frequencies, showing great potential applications in the fields of security detection [11], spectral analysis [12], bio-sensing [13,14] and high-speed communication [15].

Terahertz SC MMs research began in 2010, Gu et al. demonstrated the unique resonance phenomenon of high temperature superconductor MMs in the terahertz frequency regime under 77 K [16]. Since then, SC MMs have received rapid growing interest. Compared to microwave frequencies, SC MMs are more urgently needed in the terahertz regime because: 1) as the resonance frequency is pushed higher from microwave, the remarkable ohmic dissipation has a negative impact on device performance, 2) the intrinsic complex conductivity of SCs strongly depends on external magnetic/electric field, optical stimulation and temperature modification. Therefore, active MMs integrated with SC elements overcome the lack of functioning devices in the terahertz regime. By now, terahertz SC MMs have been demonstrated by both traditional and high temperature SCs. Various active modulations of terahertz MM devices made from SCs have been established, including the unique terahertz nonlinear SC MMs.

In this review, we systematically elaborate experimental demonstrations of terahertz SC MMs, the tuning behaviors of their resonance performance, and theoretical understanding of their unique performances based on two-fluid model and transmission line model. The presentation is organized as follows: in Section 2, we introduce several initial experimental efforts on terahertz SC MMs; in Section 3, the physical mechanism of the SC MMs is investigated; in Section 4, we discuss a number of active terahertz MM devices based on the tunability of SCs; in Section 5, we illustrate enhanced nonlinearity effect induced by intense terahertz field in SC MMs made from NbN thin film. Finally, it is concluded with the future development tendency in SC MMs in Section 6.

2 Terahertz superconducting metamaterials

The first superconductor MMs were made from high transition temperature superconductor (HTS) yttrium barium copper oxide (YBCO). In 2010, Gu and coworkers first demonstrated temperature dependent resonance performance of split ring resonators (SRRs) made from YBCO [16]. The HTS MMs, as shown in Fig. 1, were fabricated on sapphire substrate by using conventional lithography methods and wet etching process. The MM sample was lithographically fabricated from a commercially available 280-nm-thick YBCO film printed on a 500 μm thick sapphire substrate. Using a terahertz time-domain spectroscopy system integrated with a cryogenic chamber cooled by liquid helium, the temperature dependent transmission of the YBCO MM with polarization of incident electric field parallel to the SRR gap was measured, as illustrated in Fig. 2.

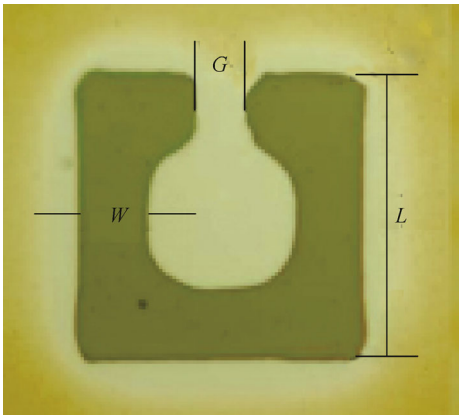

Fig. 1 Microscopic image of YBCO SRR with structure parameters: W = 8 μm. G = 5 μm, L = 32 μm and P = 52 μm [16]

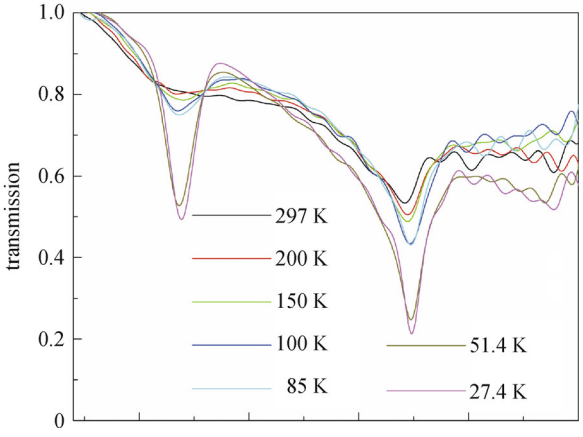

Fig. 2 Measured amplitude transmission spectra of YBCO MM at different temperatures [16]

The introduced terahertz field stimulates the circulating current in the SRRs at lower frequency generating the inductance-capacitance resonance and linear current at higher frequency giving rise to the quadrupole resonance [17–19]. At room temperature, the LC and quadrupole resonances of the YBCO SRR array, at 0.65 and 1.75 THz, respectively, appear to be quite weak due to low conductance of YBCO. When the temperature decreases down toward critical temperature (T_c), the resonance becomes more remarkable because of the increased current flow in the SC film. The resonance indicates a switching effect as the temperature crossing T_c. When the tempera-

ture is well below T_c, further cooling does not enhance the resonance much again. Comparing to the obvious amplitude switching effect of the resonance, the frequency shift is nearly neglectable. Since the temperature dependent properties of YBCO could be the only possible reason, all the modulation of the terahertz transmission originates from the superconductivity in SC MMs.

The advantage of HTS is their relatively high T_c. At 4.2 K, however, traditional superconducting metal such as Nb has an efficient surface resistance lower than that of YBCO thin film by one order of magnitude at least up to 0.3 THz [20]. Encouraged by this benefit, Jin et al. demonstrated the terahertz MMs integrated with Nb structures [21]. The fabricated SC MM chose double-split-ring-resonators (DSRR) as the unit cell as shown in the inset of Fig. 3 [22,23]. The outer and inner rings measure 120 μm × 120 μm and 80 μm × 80 μm, respectively. All of the widths of the rings, the distance between lines, and the split gaps are equal to 10 μm. The whole unit cell has a periodicity of 140 μm in both directions. The structures were fabricated from a Nb film sitting on 400-μm-thick silicon substrate. The measured transmission spectra at 6 and 26 K in two frequency ranges, i.e., 0.10 to 0.18 THz and 0.30 to 0.55 THz, were plotted as the red squares and blue circles in Fig. 3 with the fitting results represented by the solid lines, respectively. It is shown that the value of quality factor in the SC SRR array can be greatly increased as the Nb film is in the superconducting state. There are significant resonance dips observed respectively at 0.132 and 0.418 THz at 6 K in the transmission spectrum, while at 26 K both resonances shrink obviously. This is because that superconducting Nb film has a lower surface resistance than that in normal state. This work is of great significance to implement MM design with low temperature superconductor Nb.

3 Modeling of terahertz superconducting MMs

The temperature dependent response in SC MMs primarily originates from the tuning of complex conductivity in the superconducting film above and well below T_c. In 2010, Chen and coworkers proposed a theoretical model that qualitatively illustrates the temperature tuning mechanism of SC MMs [24]. A superconducting electric split-ring resonator (eSRR) array was fabricated with dimensions specified in the unit cell microscopic image shown in Fig. 4. The SC MM was made from 180-nm-thick YBCO film deposited on a 500 μm thick (100) $LaAlO_3$ (LAO) substrate, by using conventional photolithographic and wet etching process. Under normal incidence, the terahertz transmission spectra are shown in Fig. 5 as a function of temperature, by using an LAO substrate as the reference. These MMs exhibit interesting temperature-dependent resonance strength and frequency phenomenon.

At 20 K, as the temperature far below T_c, the YBCO MM exhibits the strongest resonance, as represented by the sharpest terahertz transmission dip with the transmission amplitude minimum of 0.05 dB located at 0.61 THz. As the temperature increases, the resonance shrinks, gradually broadening and reduction in amplitude of the transmission dip was observed. The resonance frequency red shifts to a lowest value of 0.55 THz near 84 K, giving rise to a 10% frequency tuning. As the temperature continues to increase, the resonance further decreases. But in contrary to the amplitude monotonic decreasing, the resonance frequency moves back to the higher frequencies. Contribution of the LAO substrate to the MM resonance modulation is excluded. The temperature-dependent properties of the YBCO film are responsible for the observed MM resonance tuning phenomenon.

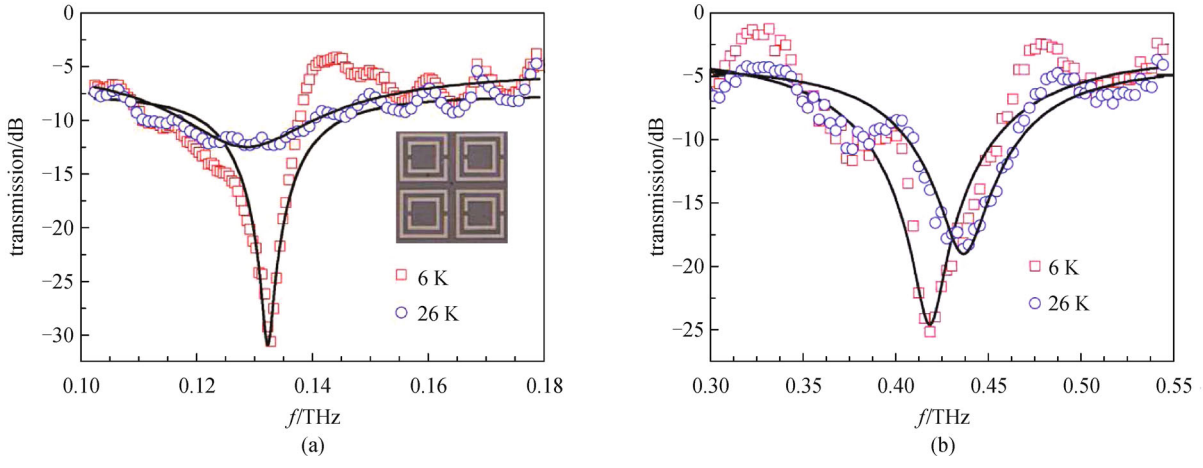

Fig. 3 Amplitude transmission spectra at 6 and 26 K for two resonance modes at (a) 0.132 and (b) 0.418 THz, respectively. The solid lines indicate the fitting results to the experiment data. Inset: Microscopic image of MM sample with the incident electric field parallel to the gap [21]

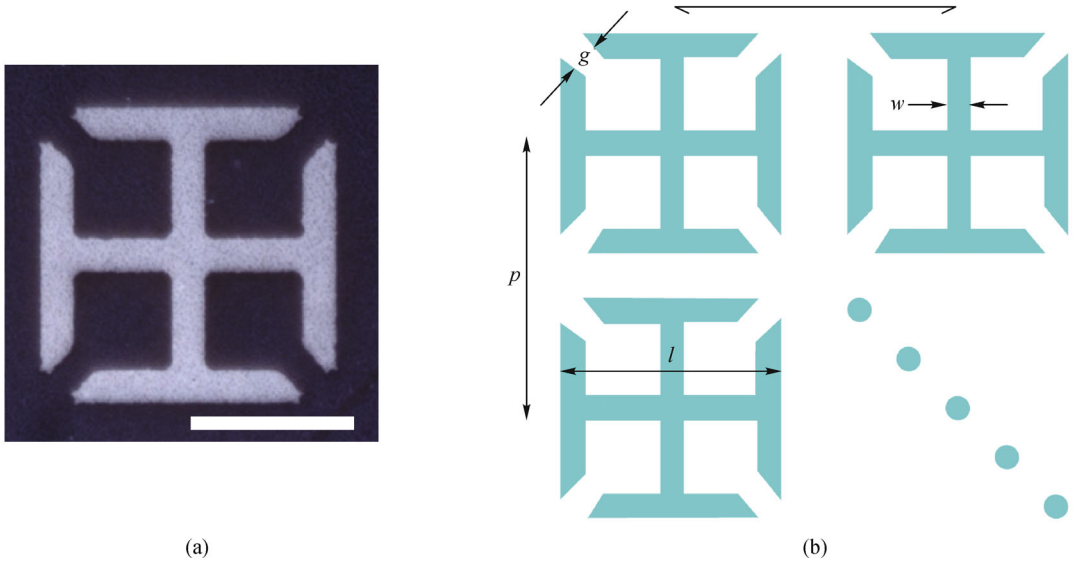

Fig. 4 (a) Micrograph of a representative eSRR. The light and black areas are YBCO film and the LAO substrate, respectively; (b) dimensions of eSRR are $g = 4$ μm, $w = 36$ μm, $l = 36$ μm, and $p = 46$ μm [24]

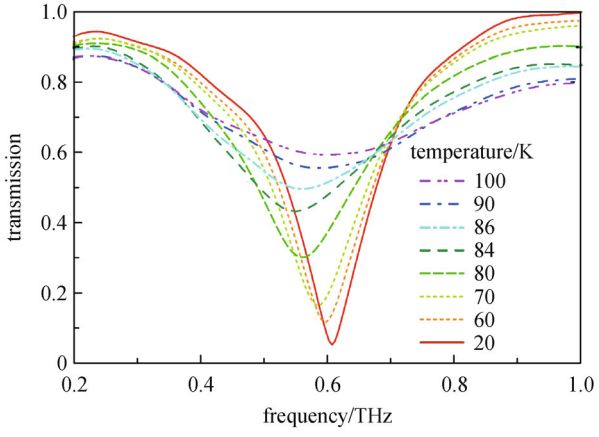

Fig. 5 Terahertz transmission spectra of a 180-nm-thick YBCO eSRR array at various temperatures [24]

To explain this temperature dependence, two-fluid model is adapted to depict the complex conductivity of SCs [25]:

$$\sigma_{\mathrm{re}} = \frac{ne^2}{m^*}\frac{f_{\mathrm{n}}(T)\tau}{1+\omega^2\tau^2},$$

$$\sigma_{\mathrm{im}} = \frac{ne^2}{m^*}\left[\frac{f_{\mathrm{n}}(T)\omega^2\tau^2}{1+\omega^2\tau^2} + \frac{f_{\mathrm{s}}(T)}{\omega}\right]. \quad (1)$$

Here, f_n and f_s are the portions of the hot quasipartical carriers and superfluid electrons, respectively, n and m^* are the density and effective mass of the carriers, respectively, and τ is the normal carriers relaxation time. Two-fluid model considers the conductivity of SC to be comprised of two parts: one is expressed by Drude response corresponding to the population of normal carriers and the other part is characterized by London equation corresponding to the behavior of superconducting electrons. Therefore, the total conductivity σ is the combination of the normal conductivity and the superconducting conductivity.

By using a cryogenic sample chamber integrated time-domain spectroscopy system, Chen et al. [24] measured the transmission amplitude spectra of both the patterned eSRR array and an unpatterned 180-nm-thick YBCO plain film, respectively. The minimal transmission amplitude spectra of the MM sample and the derived real part and imaginary part of complex conductivity in the raw film at 0.6 THz are plotted as functions of temperature in Fig. 6.

As shown in the inset of Fig. 6, the real conductivity [Eq. (1)], which stems from the Drude response of normal carriers, gradually increases when the temperature decreases to about 70 K. It then decreases slightly below 70 K all the way to 50 K. In contrary, the value of imaginary conductivity is very small when the temperature is higher than T_c, due to the second term of Eq. (2), $f_s(T > T_c) = 0$. As the temperature decreases below T_c, a prompt increment of imaginary conductivity, crossing the real conductivity below 82 K is observed, resulting from the formation of superconducting electronic state .

Based on the two-fluid model, the transmittance of YBCO film with a complex conductivity σ and thickness d could be understood in terms of an equivalent transmission line model. By equating the (multiple) reflections and transmissions from the film and the transmission line model, the complex surface impedance of the unpatterned film can be expressed as

$$\tilde{Z}_{\mathrm{s}} = R_{\mathrm{s}} - \mathrm{i}X_{\mathrm{s}} = Z_0\frac{n_3 + \mathrm{i}\tilde{n}_2\cot(\tilde{\beta}d)}{\tilde{n}_2^2 - n_3^2} = \mathrm{i}\frac{Z_0}{\tilde{n}_2}\cot(\tilde{\beta}d), \quad (2)$$

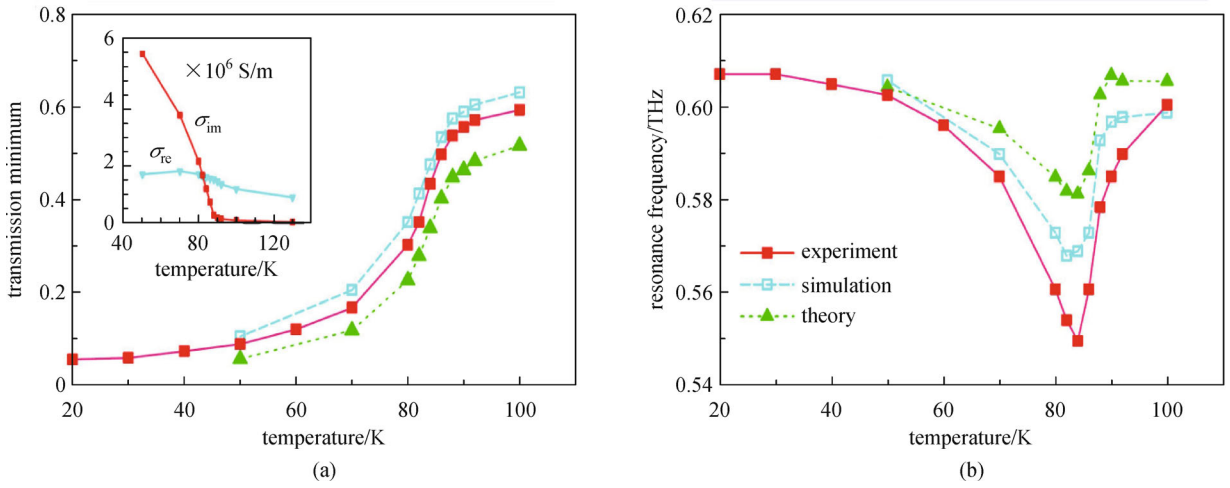

Fig. 6 (a) Minimal transmission amplitude and (b) corresponding resonance frequency at various temperatures, from experiments, numerical calculations, and theoretical simulations. The inset in (a) presents both the real and imaginary parts of the complex conductivity of the unpatterned 180-nm-thick YBCO film at 0.6 THz [24]

where the tildes above the variable parameters represent complex values, $Z_0 = 377\ \Omega$ is the vacuum impedance, n_3 is the substrate refractive index, $\tilde{n}_2 = \sqrt{i\tilde{\sigma}/\varepsilon_0\omega}$ is the complex refractive index of the film, $\tilde{\beta} = \tilde{n}_2\omega/c_0$ is the complex propagation constant. It is obvious that both the real and imaginary parts of $\tilde{\beta}$, therefore $\tilde{\sigma}$ attribute to the film surface resistance R_s and reactancef X_s. Additionally, considering the non-uniform current distribution in a elementary cell, then the SC SRR array resistance R can be acquired: $R = [(A-g)/\omega]R_s$, where A is the average circumference of the small current loop. The incremental SRR resistance R is responsible for the resonance damping, hence the transmission minimum increases as the temperature goes higher. The eSRR array could be modeled as a lumped resistor R in the transmission line, and then the resonance transmission can be calculated as a function of temperature, as shown in Fig. 6(a). It is obvious that the calculated transmission is well in consistence with the experimental and simulated results.

If an additional inductance L_s from eSRRs is taken into account besides the geometric inductance L_g, the shifting of temperature-dependent resonance frequency can also be interpreted in this transmission line model. The frequency of fundamental resonance in SRRs is given by

$$\omega_0^2 = \frac{1}{LC} - \frac{R^2}{4L^2}, \tag{3}$$

where R is resistance in eSRRs, C is the effective capacitance, and L is the total inductance, e.g., $L = L_s + L_g$. This is the combination of the geometry inductance of the SRR L_g and the additional inductance L_s coming from the kinetic inductance of the eSRRs [26]. By using the obtained YBCO film surface reactance X_s and considering the dimensions and geometry of the SRR, L_s can be derived: $L_s = [(A-g)/\omega](X_s/\omega)$, therefore, using Eq. (3), one can calculate the temperature-dependent resonance frequency of the YBCO MMs. Figure 6(b) presents the measured corresponding resonance frequency vs the temperatures, along with both numerical simulations and theoretical calculations results.

Recently, there are several works pointing out that the surface resistance R_s of SC terahertz MMs fabricated from YBCO film could be larger than that of copper with temperature of 10 K and frequency at 0.5 THz and R_s also increase with the frequency even faster when compared to copper. However, different from HTS films, the low temperature SCs, e.g., Nb, NbN, having lower real part conductivity and therefore lower ohmic loss, attracting more and more attention in terahertz MMs. In 2011, Zhang and Wu et al. found that low temperature superconducting NbN film could work at higher frequency due to its higher gap frequency $f_g = 2\Delta_0/h = 1.18$ THz, where Δ_0 is the energy gap around 0 K and h is the Plank constant [27,28]. Though they also used transmission line theory to calculate the transmission of the SC MMs, the complex conductivity of the low temperature SC was described in the framework of the BCS theory instead of two fluid models [29]. The temperature dependence of the NbN MMs is in accordance relatively well with their calculation, proving the accuracy of the estimation of R_s based on the BCS theory.

4 Active superconducting terahertz MMs

As well known, the SC in superconducting state is extremely sensitive to external perturbations, such as temperature, optical excitation, magnetic field and electrical current [30], providing opportunity to realize strong resonance tuning in the SC MMs. In fact, nearly every

report about terahertz SC MMs involves at least one type of active tuning approaches of the MM sample. These experimental demonstrations clearly promote a promising application of SC MMs as novel terahertz modulators or switches.

With no doubt, the most obvious tuning method of a SC based multifunction device is thermal tuning. As mentioned in Section 1, Gu and coworkers investigated the response of YBCO MMs as a function of temperature at terahertz frequencies and demonstrated the efficient switching effect around the transition temperature, as shown in Fig. 2. As explained in Section 2, the temperature modulation of terahertz transmission in the MMs primarily originates from the temperature-dependent conductivity in the SC MMs. When temperature gets higher than T_c, the real part of the conductivity is dominant since the absolute value of the imaginary conductivity is three orders of magnitude less than that of the real part. However, the conductivity is purely imaginary due to the creation of high density superfluid Cooper pairs as the temperature goes down below T_c. So the current in SRRs grows stronger due to the superconducting carriers and results in a sharp switching at LC and quadrupole resonances. This work also reveals that at 27.4 K, the LC and quadrupole resonances could reach as low as 0.49 and 0.21 dB with Q factors of 5.3 and 14.5, respectively. Taking example of their work, we would develop low loss active terahertz MMs with SRRs supporting superior high Q value.

Besides temperature controlling of SC MM performance, other modulation methods have also been demonstrated in superconducting terahertz MMs. For example, Singh and coworkers had established the ultrafast dynamic tuning operation on picoseconds timescale in YBCO SRRs excited by near infrared femtosecond laser pulse [31]. The HTS MMs, consisting of an eSRRs square array with dimensions specified in a unit cell shown in the inset of Fig. 7, are fabricated from epitaxial YBCO films grown by using pulsed laser deposition on LAO substracts. The transmitted terahertz signals through the YBCO MM with a thickness of 100 nm at various time delay between the femtosecond infrared excitation and terahertz probe pulses at 20 K are shown in Fig. 7, for 50 and 300 mW optical pump powers, respectively.

At low temperatures, a lower transmission of terahertz radiation is observed, since the highly superconducting YBCO film leads to the strong resonant response in the MM structure. With the introduced photo excitation, even higher photon energy is sufficient to break up the superfluid Cooper pairs into quasiparticles, resulting in significant reduction of both the conductivity and resonance, hence the measured terahertz peak transmittance is increased beginning from the pump-probe time delay located at zero, as plotted in Fig. 7. Then about 2 ps rise time occurred mostly due to time duration of the terahertz pulses, which will drastically limit the time resolution. As the pump-probe time delay continues to increase, the

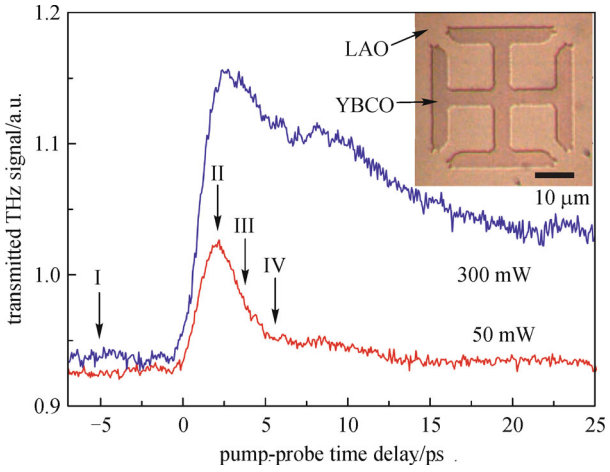

Fig. 7 Terahertz transmission of 100-nm-thick YBCO MMs exposed to near infrared femtosecond pump. The terahertz peak transmission is shown as a function of pump-probe time delay at 20 K with photoexcitation power of 50 and 300 mW. At Position I, the terahertz probe pulse arrives about 5 ps earlier than the optical pulse. It has lower transmission due to strong resonant response of the metamateria. Positions II, III and IV indicate various pump-probe time delays between the terahertz pulse and optical excitation. Inset: microscopic image of a 100-nm-thick YBCO MM unit cell. Besides, the incident terahertz pulse has the electric field polarization along the arm of SRR for all measurements [31]

measured transmitted terahertz signal amplitude decreases for the creation of superfluid Cooper pairs resulting from the recombination of quasiparticles.

The terahertz transmission amplitude spectra for the 100-nm-thick MM sample are illustrated at 20 K with different photoexcitation powers at four time delays in Fig. 8. When the terahertz pulses pass through the MM sample a few picoseconds earlier than the optical pump pulses (time position I in Fig. 7), the resonant transmission spectra for various pump powers is shown in Fig. 8(a). The tiny resulting change shows that the photoexcitation in the YBCO MM has the minimal effect. Instantly following the near infrared femtosecond pump (time position II), with increasing pump power, the MM resonance is weakened significantly and red-shifts, as shown in Fig. 8(b). Finally, the resonance dip disappears as the pump power arrives at 100 mW. The recovery of MM resonance strength as the pump-probe time interval increases because of carrier relaxation, as indicated in Figs. 8(c) and 8(d) at positions III and IV, respectively, both of them are prior to the arrival of the reflected optical excitation pulse coming back from the surface of the substrate.

It is known, accelerative supercurrent term can be strongly influenced by magnetic fields. Every superconductor has a critical magnetic field to maintain the superconducting state. Therefore, it is a quite straight way to control the SC MMs through magnetical tuning method. Jin et al. verified that magnetic tuning of Nb MMs could achieve larger quality factor of the resonance modes as the

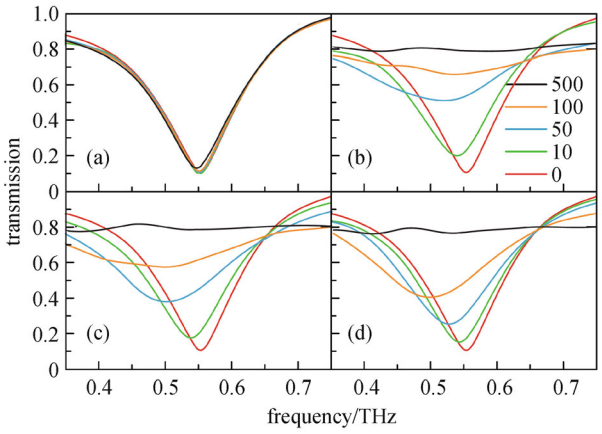

Fig. 8 Transmitted terahertz amplitude spectra of YBCO MMs as a function of various photoexcitation powers. The transmission curves shown in (a)–(d) are corresponding to the respective pump-probe time delay positions I–IV [31]

temperature below T_c in their first terahertz SC MM demonstration. Terahertz amplitude transmission experiments are conducted by using continuous-wave terahertz spectroscopy system accompanied by the necessary DC magnetic field, H_{dc}, which is provided by a superconducting split-coil magnet. e.g., $E_{in} = E_0/16X_sL_g$.

Figures 9(a) and 9(b) reveal the amplitude transmission spectra for two resonance mode curves at 6 K under various magnetic fields (0–1 T). In Fig. 9(a), with the increase of the magnetic field, both the two resonance modes decrease and the shift of the transmission vs frequency until 0.7 T can be clearly seen. Above the upper critical field, all the transmission spectra tend to keep the same and the resonance frequencies stop further shift. The physical interpretation of the tuning mechanism is that the superconducting properties of the Nb film, for instance, the magnetic penetration depth and critical current density, are strongly dependent on H_{dc} [32,33]. As H_{dc} is large above the critical field, superconductivity is quenched and the thin film becomes normal.

Besides the SRR unit cell, other structures were also explored in tunable SC terahertz devices. One example is the SC spoof surface plasmons (SSPs) structure working in terahertz regime. According to recent studies, semiconductors could show remarkable plasmonic properties and their surface plasmon (SP) frequencies mostly located in the terahertz regime, making semiconductors efficient materials for active control of the surface plasmon resonance [34–36]. For SC MMs consisting of subwavelength hole arrays, plasmonic properties and extraordinary transmission at both millimeter frequencies and terahertz regime have been discussed [37,38]. In 2011, Tian et al. demonstrated a periodic array of sub-wavelength holes made from YBCO with active thermal control method over the extraordinary transmission [36]. The chosen MM, made from a commercial 280-nm-thick YBCO film with geometric dimensions in a unit cell shown in Fig. 10, is grown on a 500-μm-thick sapphire substrate. The normalized amplitude transmission response of the YBCO array at various temperatures between 297 and 51.4 K is measured and depicted in Fig. 11.

Two resonance modes at frequencies of 0.85 and 1.16 THz with peak amplitudes transmissions of 0.69 and 0.51 dB are observed, respectively, corresponding to the $[\pm1,0]$ and $[\pm1,\pm1]$ modes of SSPs. When the SC MM is cooled down, both resonances become gradually pronounced, and their corresponding peak transmissions increase respectively. Finally, at a temperature below T_c, e.g., 51.4 K, the $[\pm1,0]$ resonance mode with the peak amplitude value arriving at nearly 0.97 dB, revealing a prominent switching effect. The significant increase of

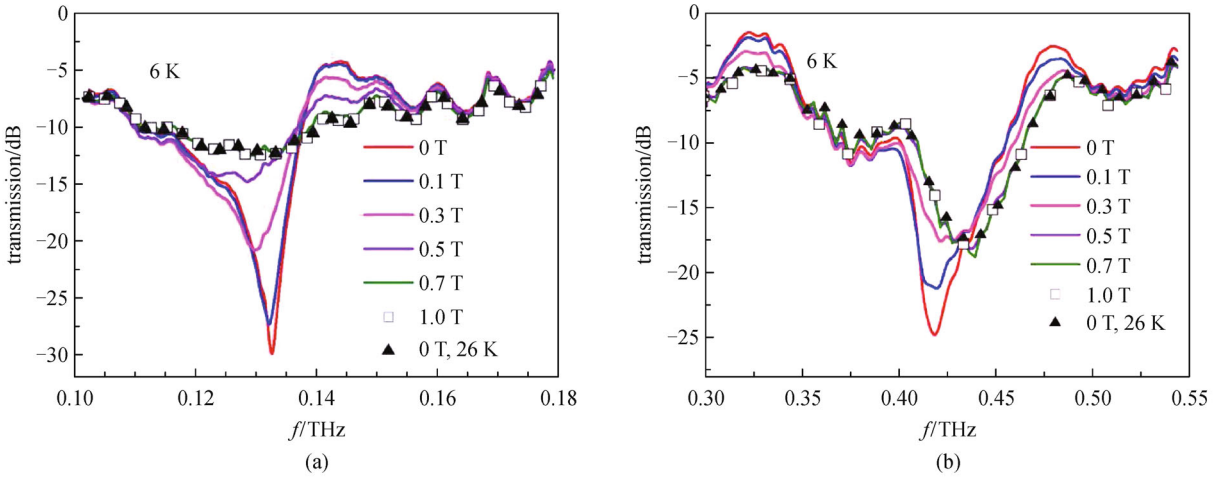

Fig. 9 Transmission vs frequency (solid lines) at 6 K with various H_{dc} = 0, 0.1, 0.3, 0.5 and 0.7 T (started from bottom) at (a) 0.132 and (b) 0.418 THz. The square symbols represent the transmission spectra at 6 K with H_{dc} = 1 T and the solid triangle symbols represent the transmission spectra at 26 K with zero H_{dc} [21]

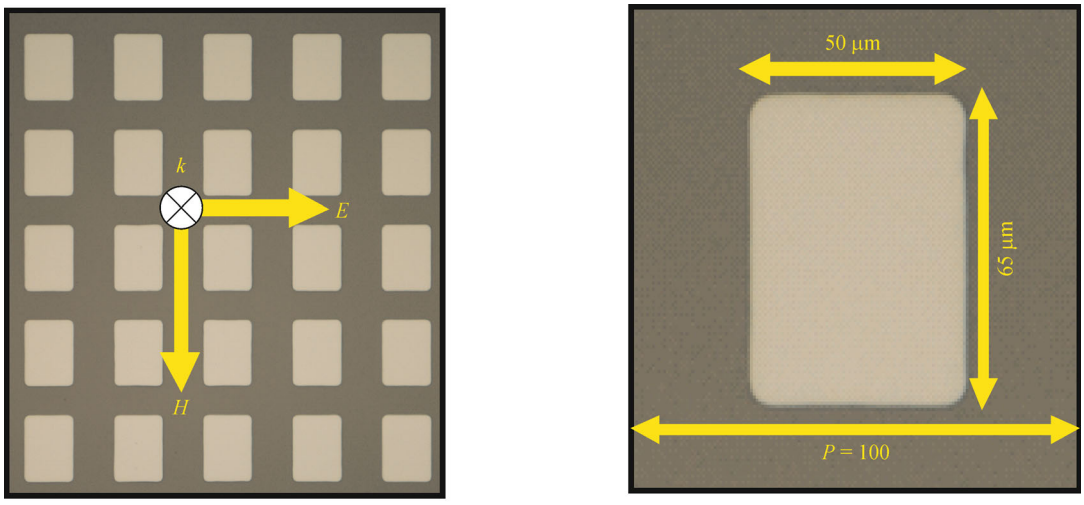

Fig. 10 Microscopic images of (a) subwavelength YBCO hole array on a sapphire substrate with a periodicity of P = 100 μm and (b) schematic diagram of an SRR unit cell with structural parameters [36]

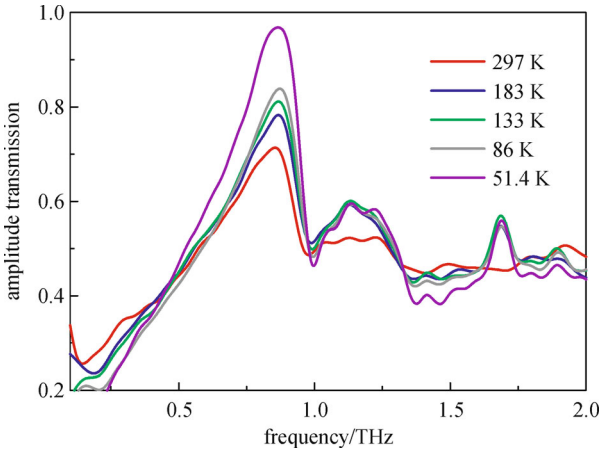

Fig. 11 Measured amplitude transmission spectra of the YBCO MM at 297, 183, 133, 86, and 51.4 K at normal incidence [36]

transmission amplitude value originates from the formation of superfluid Cooper pairs well below T_c.

In this work, an active thermal control approach over the terahertz resonant response have been achieved in a planar array of sub-wavelength YBCO holes, the remarkable amplitude modulation and sharp resonance enhancing were been seen through the transmission spectra via cooling SC MM down toward temperatures well below T_c. This type of plasmonic superconducting constructures would provide promising approaches for future design and development of amplitude modulator or thermal controlled terahertz functionality devices with low dissipation and large dynamic range.

Plasmonic-induced transparency is another broadly studied MM structure [4]. By the strong coupling between two adjacent meta-atoms, the transmission spectrum mimics electromagnetically induced transparency (EIT) – a quantum effect with very high group refractive index. Wu and coworkers designed and fabricated superconducting niobium nitride (NbN) integrated MMs structure mimicking the EIT system [39]. The schematic of the planar terahertz MMs, with geometry dimensions illustrated in Fig. 12, was proposed to imitate a three-level EIT system, where the dark and radiative resonators were both comprised of superconducting NbN thin films. From Fig. 12(a), it is obvious that each EIT-like MM unit cell includes a dark and a radiative resonator. The right-side straight metal stripe performs as a dipole antenna and has strong coupling with the incidence wave, and this straight metal stripe serves as the radiative resonator, while the double-gap split ring resonator (DSRR) acts as the dark resonator. The two resonators are designed closely enough to each other for effective coupling.

The terahertz transmission spectra of the EIT-like MM, as shown in Fig. 12(b), were measured using terahertz time-domain spectroscopy system. A typical EIT-like spectral response with a pronounced transparency window positioned between two divided resonance dips is observed. What more important is that this EIT-like response feature can be tuned by temperature. As the temperature goes down from 16 to 8 K, both the two sharp resonance dips become even strengthening and the transmission window gradually rises. Meanwhile, the frequency tuning behaviors of both the resonance dips and the transparency window with the variable temperature are also shown in Fig. 12(b).

This temperature dependence in the EIT-like transmis-

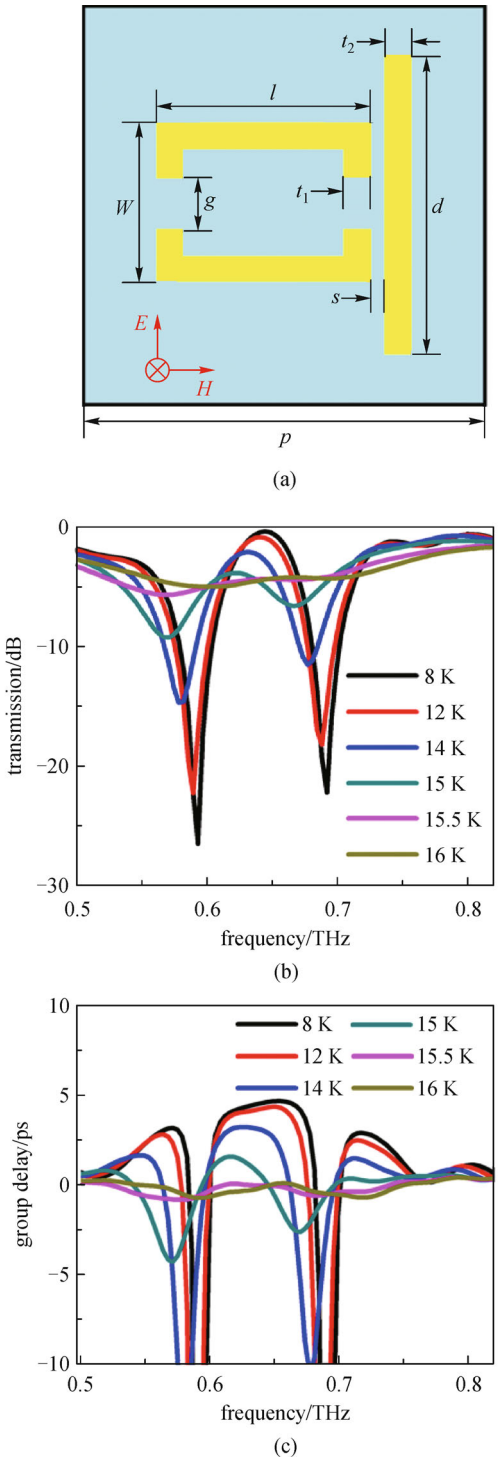

Fig. 12 (a) Schematic of the three-level EIT-like MM. The geometric parameters are $p = 120$ μm, $l = 64$ μm, $W = 48$ μm, $s = 4$ μm, $t_1 = t_2 = 8$ μm, $g = 15$ μm, $d = 90$ μm. The incident direction and the polarization of the electric field was also indicated; (b) transmission spectra for the three-level EIT-like MM at various temperatures; (c) calculated group delay vs frequency at various temperatures [39]

sion spectra can be understood as follows: 1) the higher amplitude transmission benefits from the strengthened coupling between the radiative and dark resonators in the superconducting state [4]; 2) the transmission at the transparency window increased due to reduced ohmic dissipation in the dark resonators. Thus, the group delay, e. g., the group refractive index of the EIT-like MM also experiences a monotonic increase as the temperature reduces, as shown in Fig. 12(c). The high transmission combined with wideband tuning properties and large delay-bandwidth product at the transparency window of the superconducting EIT-like MMs enable promising terahertz functional applications.

5 Nonlinear response of superconducting metamaterials

As mentioned above, SC is utilized as a new approach to manipulate the response of terahertz MMs. Until now, however, all terahertz MMs have been working in a linear domain. The notation of MMs can actually be extended to the nonlinear regime if the elements are formed from or contain nonlinear components [40]. In the past few years, the rapid development of high terahertz intensity technology enables to yield field strength reaching a few hundreds of KV/cm. The terahertz radiation based on the titled-pulse-front optical rectification in $LiNbO_3$ can be generated with field intensity up to several MV/cm. The record high intensity source delivers availability for observing and exploring ultrafast dynamic nonlinear phenomena in the terahertz MMs.

Recently, Zhang et al. have explored nonlinear response of a terahertz MM consisting of SRRs made from NbN under intense incident terahertz field [40,41]. The MM is a planar array of superconducting NbN SRRs periodically deposited on a 1-mm-thick MgO substrate with the incident field polarization perpendicular to the gap of the

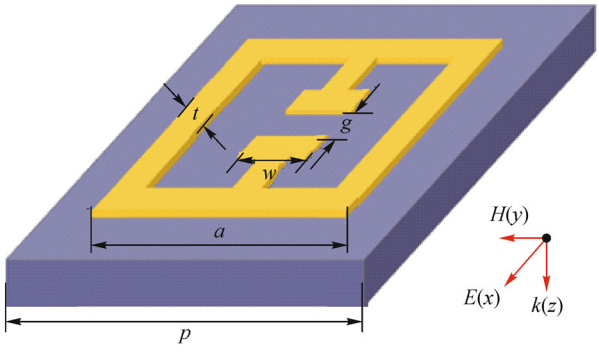

Fig. 13 Schematic of the SC MM unit cell with structural parameters: $g = t = 5$ μm, $w = 10$ μm, $a = 50$ μm, and a periodicity of $P = 60$ μm, where E and H represent the electric field and magnetic field, respectively [40]

SRRs. The schematic of the SC MM unit cell with geometrical parameters is illustrated in Fig. 13. A typical LC resonance is stimulated and the normalized amplitude transmission spectra are measured with different incident terahertz field strength at 4.5 K, as shown in Fig. 14.

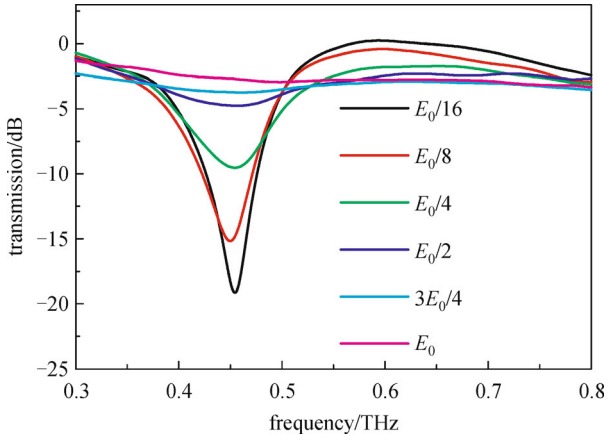

Fig. 14 Measured amplitude transmission spectra for the SC MM with various incident terahertz field strengths at 4.5 K [40]

As incident field strength is low, e.g., $E_i = E_0/16$, the transmission response presents a sharp resonance dip reaching −20 dB at about 0.45 THz, and E_i is too weak to cause the remarkable nonlinearities. Then, as the incident terahertz electric field increases from $E_0/16$ to E_i, the resonant transmission dip experiences a reduction from −20 to −3 dB with a small change in the resonance frequency. Finally, at $E_{in} = E_0$, the fundamental LC resonance dip is remarkably reduced and even disappeared. As a result, one would expect a substantial variation in the transmission spectra by increasing the strength of incident terahertz electric field, which is ascribed to the nonlinearity of the integrated SC NbN components.

The intrinsic conductivity of the superconducting film which associates to the density population of the superfluid Cooper pairs and normal carriers plays a crucial role in the resonance property tuning of the SC MMs [41]. The real and the imaginary parts extracted from the measured complex conductivity of the 50-nm-thick NbN film at various terahertz filed strengths are shown in Fig. 15, respectively.

The density of the superfluid Cooper pairs could be modified by the introduced high intensity terahertz field, therefore the real part of the complex conductivity in the SC film increases and the imaginary conductivity was significantly suppressed with the increasing terahertz electric field [42,43], which reasonably matches the famous two-fluid model. By ignoring the thermal effect induced by intense terahertz radiation, the switchable functionality is acquired due to nonlinear response of the MM, in which the complex conductivity of the lumped SC NbN elements will change as the induced terahertz field strength varies. The performance of the SC MM can been taken as a RLC circuit model equivalently [44], in which the amplitude transmission is associated with the effective surface resistor R and the resonance frequency relies on the kinetic inductance L_k. Using the measured complex conductivity, the values of effective surface reactance $X_s = \omega L_k$ and resistance R_s of the NbN film at 4.5 K as a function of the incident terahertz electric field strength are obtained, as shown in Fig. 16.

The $R_{s,eff}$ exhibits a dramatical increase as E_{in} increases

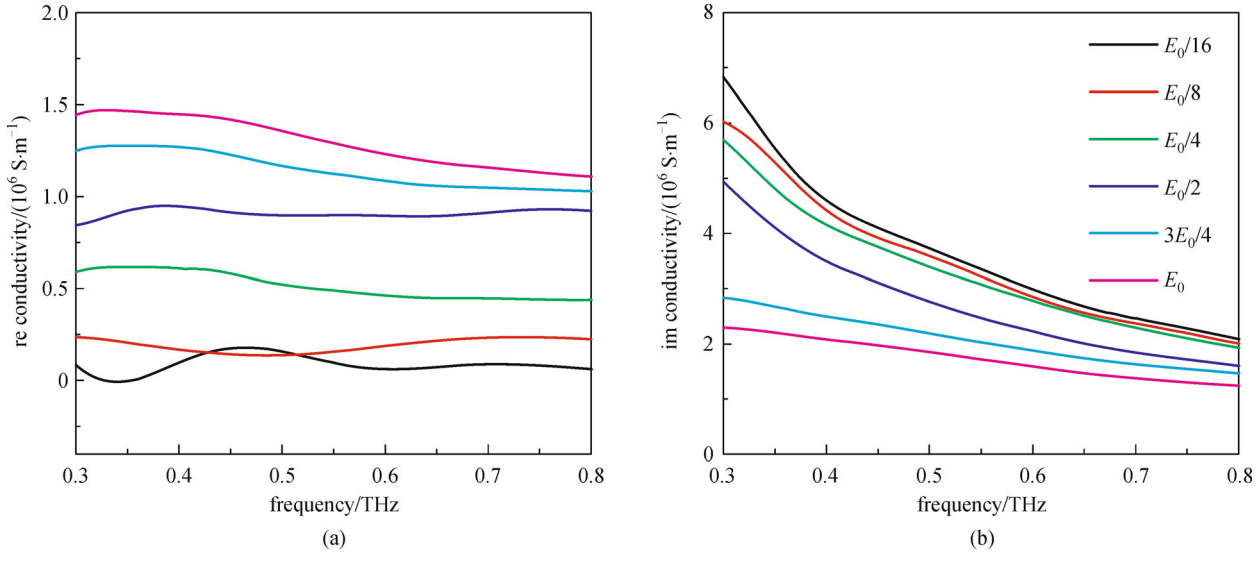

Fig. 15 Real (a) and imaginary (b) conductivities of 50-nm-thick NbN thin film with different incident terahertz field strengths [40]

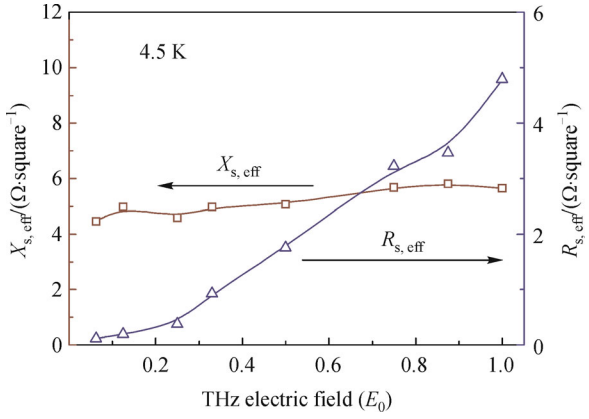

Fig. 16 Effective surface reactance $X_{s,eff}$ and resistance $R_{s,eff}$ of the SC NbN film located at resonance frequency 0.45 THz with various incident terahertz field intensity from measured complex conductivity at 4.5 K [40]

and gives rise to a prominent reduction of the resonance dip. On the other side, $X_{s,eff}$ (L_k) maintains almost invariant due to the compensation between the increase of the density of normal quasiparticles (strengthen the screening capability to E_{in}) and the reduction of the density of the superfluid Cooper pairs (strengthen the penetration of E_{in}). Consequently, the resonance frequency of the SC MM remains almost invariant since L_g and C are nearly unchanged under varying E_{in}. The nonlinear response observed in the SC MMs is not only useful in developing active and nonlinear terahertz devices, but also enables approach to exploit the physical mechanisms of nonlinear phenomena.

6 Conclusion

We have reviewed the resonance behavior manipulation with respect to both resonance frequency and amplitude in SC MMs under optical, thermal, and magnetic switching. By utilizing the two-fluid-model and equivalent resistor-inductor-capacitor circuit theory, we further elucidated the fascinating resonance phenomena in the SRR structures by taking into account of the unit cell resistance and additional inductance. These superconducting MMs that are labeled with low loss and extremely sensitive to exotic stimulations would be useful in realizing active multifunctional terahertz MMs and nonlinear devices.

Acknowledgements This work was supported by the National Basic Research Program of China (No. 2014CB339800), the National Natural Science Foundation of China (Grant Nos. 61107053 and 61138001), the Major National Development Project of Scientific Instruments and Equipment of China (No. 2011YQ150021), and the U.S. National Science Foundation (Grand No. ECCS-1232081).

References

1. Pendry J B. Negative refraction makes a perfect lens. Physical Review Letters, 2000, 85(18): 3966–3969
2. Fang N, Lee H, Sun C, Zhang X. Sub-diffraction-limited optical imaging with a silver superlens. Science, 2005, 308(5721): 534–537
3. Shelby R A, Smith D R, Schultz S. Experimental verification of a negative index of refraction. Science, 2001, 292(5514): 77–79
4. Zhang S, Genov D A, Wang Y, Liu M, Zhang X. Plasmon-induced transparency in metamaterials. Physical Review Letters, 2008, 101 (4): 047401
5. Gansel J K, Thiel M, Rill M S, Decker M, Bade K, Saile V, von Freymann G, Linden S, Wegener M. Gold helix photonic metamaterial as broadband circular polarizer. Science, 2009, 325 (5947): 1513–1515
6. Schurig D, Mock J J, Justice B J, Cummer S A, Pendry J B, Starr A F, Smith D R. Metamaterial electromagnetic cloak at microwave frequencies. Science, 2006, 314(5801): 977–980
7. Pendry J B, Schurig D, Smith D R. Controlling electromagnetic fields. Science, 2006, 312(5781): 1780–1782
8. Zheludev N I. Applied physics. The road ahead for metamaterials. Science, 2010, 328(5978): 582–583
9. Ricci M, Orloff N, Anlage S M. Superconducting metamaterials. Applied Physics Letters, 2005, 87(3): 034102
10. Fedotov V A, Tsiatmas A, Shi J H, Buckingham R, de Groot P, Chen Y, Wang S, Zheludev N I. Temperature control of Fano resonances and transmission in superconducting metamaterials. Optics Express, 2010, 18(9): 9015–9019
11. Tonouchi M. Cutting-edge terahertz technology. Nature Photonics, 2007, 1(2): 97–105
12. Ferguson B, Zhang X C. Materials for terahertz science and technology. Nature Materials, 2002, 1(1): 26–33
13. O'Hara J F, Singh R, Brener I, Smirnova E, Han J, Taylor A J, Zhang W. Thin-film sensing with planar terahertz metamaterials: sensitivity and limitations. Optics Express, 2008, 16(3): 1786–1795
14. Debus C, Bolivar P H. Frequency selective surfaces for high sensitivity terahertz sensing. Applied Physics Letters, 2007, 91(18): 184102
15. Kleine-Ostmann T, Nagatsuma T. A review on terahertz communications research. Journal of Infrared, Millimeter, and Terahertz Waves, 2011, 32(2): 143–171
16. Gu J, Singh R, Tian Z, Cao W, Xing Q, He M, Zhang J W, Han J, Chen H T, Zhang W. Terahertz superconductor metamaterial. Applied Physics Letters, 2010, 97(7): 071102
17. Singh R, Tian Z, Han J, Rockstuhl C, Gu J, Zhang W. Cryogenic temperatures as a path toward high-Q terahertz metamaterials. Applied Physics Letters, 2010, 96(7): 071114
18. Singh R, Smirnova E, Taylor A J, O'Hara J F, Zhang W. Optically thin terahertz metamaterials. Optics Express, 2008, 16(9): 6537–6543
19. Singh R, Azad A K, O'Hara J F, Taylor A J, Zhang W. Effect of metal permittivity on resonant properties of terahertz metamaterials. Optics Letters, 2008, 33(13): 1506–1508
20. Wilke I, Khazan M, Rieck C T, Kuzel P, Kaiser T, Jaekel C, Kurz H. Terahertz surface resistance of high temperature superconducting

thin films. Journal of Applied Physics, 2000, 87(6): 2984–2988
21. Jin B, Zhang C, Engelbrecht S, Pimenov A, Wu J, Xu Q, Cao C, Chen J, Xu W, Kang L, Wu P. Low loss and magnetic field-tunable superconducting terahertz metamaterial. Optics Express, 2010, 18 (16): 17504–17509
22. Azad A K, Dai J, Zhang W. Transmission properties of terahertz pulses through subwavelength double split-ring resonators. Optics Letters, 2006, 31(5): 634–636
23. Pendry J B, Holden A J, Robbins D J, Stewart W J. Magnetism from conductors and enhanced nonlinear phenomena. IEEE Transactions on Microwave Theory and Techniques, 1999, 47(11): 2075–2084
24. Chen H T, Yang H, Singh R, O'Hara J F, Azad A K, Trugman S A, Jia Q X, Taylor A J. Tuning the resonance in high-temperature superconducting terahertz metamaterials. Physical Review Letters, 2010, 105(24): 247402
25. London F, London H. The electromagnetic equations of the supraconductor. Proceedings of the Royal Society of London. Series A, Mathematical and Physical Sciences, 1935, 149(866): 71–88
26. Ricci M C, Anlage S M. Single superconducting split-ring resonator electrodynamics. Applied Physics Letters, 2006, 88(26): 264102
27. Zhang C H, Wu J B, Jin B B, Ji Z M, Kang L, Xu W W, Chen J, Tonouchi M, Wu P H. Low-loss terahertz metamaterial from superconducting niobium nitride films. Optics Express, 2012, 20(1): 42–47
28. Wu J, Jin B, Xue Y, Zhang C, Dai H, Zhang L, Cao C, Kang L, Xu W, Chen J, Wu P. Tuning of superconducting niobium nitride terahertz metamaterials. Optics Express, 2011, 19(13): 12021–12026
29. Kang L, Jin B B, Liu X Y, Jia X Q, Chen J, Ji Z M, Xu W W, Wu P H, Mi S B, Pimenov A, Wu Y J, Wang B G. Suppression of superconductivity in epitaxial NbN ultrathin films. Journal of Applied Physics, 2011, 109(3): 033908
30. Purcell E M, Morin D J. Electricity and Magnetism. Cambridge: Cambridge University Press, 2013
31. Singh R, Xiong J, Azad A K, Yang H, Trugman S A, Jia Q X, Taylor A J, Chen H T. Optical tuning and ultrafast dynamics of high-temperature superconducting terahertz metamaterials. Nanophotonics, 2012, 1(1): 117–123
32. Coffey M W, Clem J R. Unified theory of effects of vortex pinning and flux creep upon the rf surface impedance of type-II superconductors. Physical Review Letters, 1991, 67(3): 386–389
33. Ricci M C, Xu H, Prozorov R, Zhuravel A P, Ustinov A V, Anlage S M. Tunability of superconducting metamaterials. IEEE Transactions on Applied Superconductivity, 2007 17(2): 918–921
34. Han J, Lakhtakia A, Tian Z, Lu X, Zhang W. Magnetic and magnetothermal tunabilities of subwavelength-hole arrays in a semiconductor sheet. Optics Letters, 2009, 34(9): 1465–1467
35. Chen H T, Lu H, Azad A K, Averitt R D, Gossard A C, Trugman S A, O'Hara J F, Taylor A J. Electronic control of extraordinary terahertz transmission through subwavelength metal hole arrays. Optics Express, 2008, 16(11): 7641–7648
36. Tian Z, Singh R, Han J, Gu J, Xing Q, Wu J, Zhang W. Terahertz superconducting plasmonic hole array. Optics Letters, 2010, 35(21): 3586–3588
37. Wu J, Dai H, Wang H, Jin B, Jia T, Zhang C, Cao C, Chen J, Kang L, Xu W, Wu P. Extraordinary terahertz transmission in superconducting subwavelength hole array. Optics Express, 2011, 19 (2): 1101–1106
38. Fedotov V A, Tsiatmas A, Shi J H, Buckingham R, de Groot P, Chen Y, Wang S, Zheludev N I. Temperature control of Fano resonances and transmission in superconducting metamaterials. Optics Express, 2010, 18(9): 9015–9019
39. Wu J, Jin B, Wan J, Liang L, Zhang Y, Jia T, Cao C, Kang L, Xu W, Chen J, Wu P. Superconducting terahertz metamaterials mimicking electromagnetically induced transparency. Applied Physics Letters, 2011, 99(16): 161113
40. Zhang C, Jin B, Han J, Kawayama I, Murakami H, Wu J, Kang L, Chen J, Wu P, Tonouchi M. Terahertz nonlinear superconducting metamaterials. Applied Physics Letters, 2013, 102(8): 081121
41. Zhang C, Jin B, Han J, Kawayama I, Murakami H, Jia X, Liang L, Kang L, Chen J, Wu P, Tonouchi M. Nonlinear response of superconducting NbN thin film and NbN metamaterial induced by intense terahertz pulses. New Journal of Physics, 2013, 15(5): 055017
42. Grady N K, Perkins B G Jr, Hwang H Y, Brandt N C, Torchinsky D, Singh R, Yan L, Trugman D, Trugman S A, Jia Q X, Taylor A J, Nelson K A, Chen H T. Nonlinear high-temperature superconducting terahertz metamaterials. New Journal of Physics, 2013, 15(10): 105016
43. Matsunaga R, Shimano R. Nonequilibrium BCS state dynamics induced by intense terahertz pulses in a superconducting NbN film. Physical Review Letters, 2012, 109(18): 187002
44. Schurig D, Mock J J, Smith D R. Electric-field-coupled resonators for negative permittivity metamaterials. Applied Physics Letters, 2006, 88(4): 041109

Xiaoling Zhang received the B. E. degree in control technology and instruments from Changchun University of Science and Technology, Changchun, China, in 2012. She is currently a graduate student at the Center for Terahertz Waves, Tianjin University, Tianjin, China, under the supervision of Profs. J. Q. Gu, J. G. Han and W. L. Zhang. Her research focuses on the generation and detection of terahertz wave radiation.

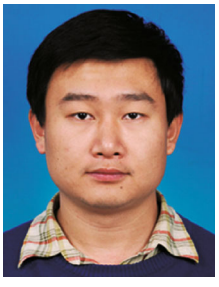

Jianqiang Gu received the B.S. degree in electronic science and technology, and the M.S. and Ph.D. degrees in opto-electronics technology from Tianjin University, Tianjin, China, in 2004, 2007, and 2010, respectively. From 2008 to 2010, he was a visiting Ph.D. candidate in the School of Electrical and Computer Engineering, Oklahoma State University, Stillwater, USA. Currently, he is on the faculty of the College of Precision Instruments and Optoelectronics Engineering, and a member of the

Center for Terahertz Waves, Tianjin University, China. His current research interests include metamaterials, surface plasmon polaritons, and material studies in the terahertz regime.

Jiaguang Han received the B.S. degree in material physics from Beijing Normal University, Beijing, China, in 2000, and the Ph.D. degree in applied physics from the Shanghai Institute of Applied Physics, Chinese Academy of Sciences, Shanghai, China, in 2006. He was a visiting researcher at the Japanese High Energy Accelerator Research Organization during 2004–2005. From 2006 to 2007, he was a Post-doctoral Researcher in the School of Electrical and Computer Engineering, Oklahoma State University, Stillwater, OK, USA. In 2007, he joined the Department of Physics, National University of Singapore, Singapore, where he was a Lee Kuan Yew Research Fellow. Currently, he is Professor in the College of Precision Instruments and Optoelectronics Engineering, and a member of the Center for Terahertz Waves, Tianjin University, China. His current research interests include surface plasmon polaritons, metamaterials, and material studies in the terahertz regime. Dr. Han is a recipient of the Einstein Award from the Embassies of Germany and Switzerland in 2006, and was invited to visit the German and Swiss universities and research institutes.

Weili Zhang received the B.S. degree in laser science, and the M.S. and Ph.D. degrees in optical engineering from Tianjin University, Tianjin, China, in 1987, 1990, and 1993, respectively. From 1993 to 1995, he was a Post-Doctoral Research Associate in the Department of Physics, The Hong Kong University of Science and Technology, Hong Kong. In 1995, he joined the faculty in the Department of Optoelectronics Technology, Tianjin University. Since 2000, he was Visiting Associate Professor, Associate Professor, and currently Professor at the School of Electrical and Computer Engineering at Oklahoma State University, Stillwater, OK, USA. He is also Professor in the College of Precision Instruments and Optoelectronics Engineering and Director of the Center for Terahertz Waves, Tianjin University, China. His research interests include terahertz optoelectronics, nanostructured and microstructured materials optics, and ultrafast lasers and phenomena. Dr. Zhang is Associate Editor of the Journal of Optoelectronics and Lasers, Guest Editor for a number of peer-reviewed journals, including IEEE Journal of Selected Topics in Quantum Electronics, and Chinese Optics Letters, and member of the editorial board of Journal of Photonics, Optoelectronics Letters, and Chinese Optics Letters. He was the general Co-Chair for the 4th International Symposium on Ultrafast Phenomena and Terahertz Waves, Tianjin, China, in 2008. He was the Session Chair and Program Committee Member for many international conferences, including CLEO, PIERS, Optics East, SPIE Defense, Security, and Sensing, and OSA topical meetings.